Received: 17 October 2023 | Revised: 4 January 2024 | Accepted: 15 January 2024

DOI: 10.1002/hbm.26609

RESEARCH ARTICLE

WILEY

The neural mechanisms of identifiable victim effect in prosocial decision-making

Hailing Zhao[1] | Yashi Xu[1] | Lening Li[2] | Jie Liu[1,3] | Fang Cui[1,3]

[1]School of Psychology, Shenzhen University, Shenzhen, China

[2]Department of Biomedical Engineering, The Hong Kong Polytechnic University, Hong Kong, China

[3]Center for Brain Disorders and Cognitive Neuroscience, Shenzhen University, Shenzhen, China

Correspondence

Jie Liu and Fang Cui, School of Psychology, Shenzhen University, Shenzhen 518060, China.
Email: ljier06@gmail.com and cuifang0826@gmail.com

Funding information

Science, Technology and Innovation Commission of Shenzhen Municipality, Grant/Award Number: JCYJ20210308103903001; National Natural Science Foundation of China, Grant/Award Number: 32171013

Abstract

The phenomenon known as the "identifiable victim effect" describes how individuals tend to offer more assistance to victims they can identify with than to those who are vague or abstract. The neural underpinnings of this effect, however, remain elusive. Our study utilized functional magnetic resonance imaging to delve into how the "identifiable victim effect" influences prosocial decision-making, considering different types of helping costs, across two distinct tasks. Participants were instructed to decide whether to help a victim with personal information shown (i.e., the identifiable victim) and an unidentifiable one by costing their money (task 1) or physical effort (task 2). Behaviorally, we observed a pronounced preference in both tasks for aiding identifiable victims over anonymous ones, highlighting a robust "identifiable victim effect." On a neural level, this effect was associated with heightened activity in brain areas like the bilateral temporoparietal junction (TPJ) when participants confronted anonymous victims, potentially indicating a more intensive mentalizing process for less concrete victims. Additionally, we noted that the TPJ's influence on value judgment processes is mediated through its functional connectivity with the medial prefrontal cortex. These insights contribute significantly to our understanding of the psychological and neural dynamics underlying the identifiable victim effect.

KEYWORDS

empathy, functional magnetic resonance imaging, identifiable victim effect, prosocial decision-making, temporoparietal junction

1 | INTRODUCTION

In real life, we do not help everyone equally since multiple factors are considered when making helping decisions. Research indicates a stronger propensity to assist identifiable victims over those who are anonymous or represented statistically (Kogut & Kogut, 2013; Kogut & Ritov, 2005; Loewenstein & Small, 2007). This bias toward victims with detailed personal information is termed the "identifiable victim effect" (Fetherstonhaugh et al., 1997; Jenni & Loewenstein, 1997). Specifically, victims with accessible personal data such as names, genders, identities, ages, and photos are deemed identifiable, whereas groups represented by statistics or descriptions are considered unidentifiable (Kogut & Ritov, 2005).

Previous studies have partially unraveled the psychological underpinnings of this effect (Hou et al., 2023). Recent findings suggest that presenting victims' photographs and names reduces the interpersonal distance between decision-makers and the victims, thereby enhancing a sense of responsibility and a willingness to donate (Kogut & Kogut, 2011; Kogut & Kogut, 2013). As Dickert et al. (2011) noted, concrete victims are more likely to induce associations, speculations, and psychological representations of their situation in the potential helpers than vague and abstract victims. Individuals developed stronger empathy for the pain of identifiable victims than unidentifiable victims (Erlandsson et al., 2015; Genevsky et al., 2013), and relaying victims' tragic experiences can further stimulate empathy and prosocial behavior (Hou et al., 2023; Lee & Feeley, 2016).

While the identifiable victim effect is well-documented behaviorally, its neural basis remains largely unexplored. Our study employed functional magnetic resonance imaging (fMRI) to investigate this effect at both behavioral and neural levels. We selected experimental materials (i.e., victims' information) from a prominent online crowdfunding platform in China. Participants were tasked with making donation decisions for either an identifiable or unidentifiable victim, involving either monetary contributions (the Money task) or physical effort (the Effort task).

Online crowdfunding, emerging as a significant philanthropic avenue, offers a novel perspective on charitable giving, marked by its scope and convenience. Compared to traditional fundraising methods, online donors usually have limited information about beneficiaries, making the presented data crucial in influencing donation decisions.

Understanding the identifiable victim effect in the context of online crowdfunding is pivotal. It may lead to resource concentration on a few visible beneficiaries, potentially causing an uneven resource distribution (Small et al., 2007). Conversely, leveraging this effect could boost helping willingness and improve fundraising outcomes (Andreoni, 1990; Harbaugh et al., 2007; Small et al., 2007). Thus, in-depth research into both the behavioral and neural mechanisms of this effect in online crowdfunding is essential.

Behaviorally, we hypothesized that participants would show a greater tendency to donate to identifiable victims, aligning with the "identifiable victim effect." On the neural level, we predicted that regions associated with affective empathy, like the insula and middle cingulate cortex (MCC), would exhibit a stronger activation when facing identifiable victims compared to the unidentifiable ones due to the higher emotional contagion and empathic concern induced by identifiable victims (Lamm et al., 2011, Singer, 2006). Conversely, confronting unidentifiable victims would demand more cognitive empathy, activating regions like the temporoparietal junction (TPJ), medial prefrontal cortex (mPFC), superior temporal sulcus, temporal pole (TP), and others (Buckner et al., 2008; Corbetta et al., 2008; Decety & Lamm, 2007; Frith & Singer, 2008; Schurz et al., 2014; Tremblay et al., 2017; Van Overwalle & Baetens, 2009; Young et al., 2007). These areas would likely influence valuation regions such as the mPFC and the striatum (Bartra et al., 2013). Furthermore, we hypothesized that the activation levels or patterns in these regions would predict the extent of the behavioral effect. Finally, we predicted that the nature of the helping cost (monetary or physical effort) would not alter the neural mechanism underlying this effect, expecting consistent results across both tasks.

2 | METHODS

2.1 | Participants

Thirty-five healthy adult participants were recruited from Shenzhen University. All participants were right-handed and had normal or corrected to normal vision. Four participants' data were excluded from analysis, two having head motion greater than 2 mm or rotation greater than 2° and the other two because of their failure to complete one of the two tasks. Data from 31 participants (15 females, 20.26 ± 1.81 years [mean ± standard deviation]) were included finally. The study was conducted according to the ethical guidelines and principles of the Declaration of Helsinki and was approved by the Medical Ethical Committee of Shenzhen University Medical School. Informed consent was obtained from all participants after they fully understood the procedures.

2.2 | Experimental design and procedure

"Waterdrop" serves as a prominent online crowdfunding platform in China, primarily focused on gathering financial support for individuals grappling with severe illnesses. Through this platform, those in need can post authenticated requests for monetary aid, and altruistic donors have the opportunity to contribute to their cause. For our experiment, we selected a series of such requests from the "Waterdrop" platform. These were meticulously chosen to maintain a balance in terms of the victims' age, gender, and identity. In our tasks, participants assumed the role of a benefactor, making donation decisions as a "decision-maker."

Our study comprised two distinct tasks conducted on separate days: the "Money Task" (task 1) and the "Effort Task" (task 2). Participants were required to return to the laboratory for the second task 1–2 weeks after completing the first. The order of these tasks was evenly distributed among participants, with 14 completing the Money Task first and 17 starting with the Effort Task.

The experiment was structured as a one-factor within-subjects design, with the factor being the "identifiability" of the victim. This factor had two levels: in the identifiable victim condition (IV condition), participants made decisions about victims whose personal information was disclosed to them. In contrast, in the unidentifiable victim condition (UIV condition), they made decisions about victims whose information was concealed.

The two tasks were only differing in terms of the costs the participants paid to be able to help the victims. Specifically, in the *Money Task*, they need to cost their own money, while in the *Effort Task* they need to perform gripping force (i.e., cost their physical effort) to enable the donation. Following is a detailed description of each task.

2.2.1 | Task 1: Money task

Participants were informed that at the beginning of each trial, they would be given 10 monetary units (MUs), which could be converted into additional real money post-experiment. They had the option to donate these MUs to the victim in the trial or keep them. For instance, if a participant chose to donate 4 MUs from the 10 allocated, they would retain 6 MUs. These retained MUs could be converted into real money, augmenting their base pay of approximately 8 dollars per hour, if the trial was selected for execution (as illustrated in Figure 1a). The exchange rate of 1 MU to 2 yuan (approximately 0.3 dollars) was disclosed to participants only at the end of the scanning session.

Each trial commenced with the presentation of two covered cards, each symbolizing a victim, displayed for 2 s. Subsequently, one card was unveiled, revealing details like age, gender, and identity of one victim (IV), while the other victim's information remained undisclosed (UIV). After a 1.5-s display of this information, one of the victims was randomly chosen for the trial's donation. If the revealed card was selected, participants knew the chosen victim's personal details (IV condition); otherwise, they decided on donations without knowledge of the victim (UIV condition). This design was intended to control information input, ensuring that any observed differences between IV and UIV conditions were not due to varying levels of physical and social inputs or social processing requirements. Here, we presented both identifiable and unidentifiable victims in each trial to control the input of information such that the difference observed between the IV and UIV conditions was not caused by different physical or social inputs (the IV condition showed meaningful words while the UIV condition did not) or the different levels of social processing (personal information need to be processed in IV condition but not in UIV condition).

During the "Chosen victim info" phase, which lasted 5 s, followed by a 0.5-s blank interval, participants indicated their donation amount via button presses on the "Decision phase". They could choose from six options (0–10 MUs in increments of 2). The selection was highlighted by changing the option's color from white to red. To avoid any priming effects, the initial position of the red label was pseudo-randomized. Participants used an MRI-compatible button box to navigate their choice and had a maximum of 3 s to respond (as shown in Figure 1b). The task comprised 120 trials, divided into four runs, with a total duration of approximately 30 min. Trials from both conditions were pseudo-randomized. Participants had a practice session of eight trials to acclimate to the tasks before the actual scanning.

It was made clear to participants that only 12 of the trials would be randomly selected for actual execution. The experimenter would donate the corresponding money (converted from the MUs allocated by participants in these trials) on behalf of the participant, while the total MUs retained by participants would be converted into real money and added to their compensation.

2.2.2 | Task 2: Effort task

Instead of using MUs, participants donated by exerting physical effort through squeezing a hand gripper. The criteria for donation were set as follows: for every two successful squeezes, participants would

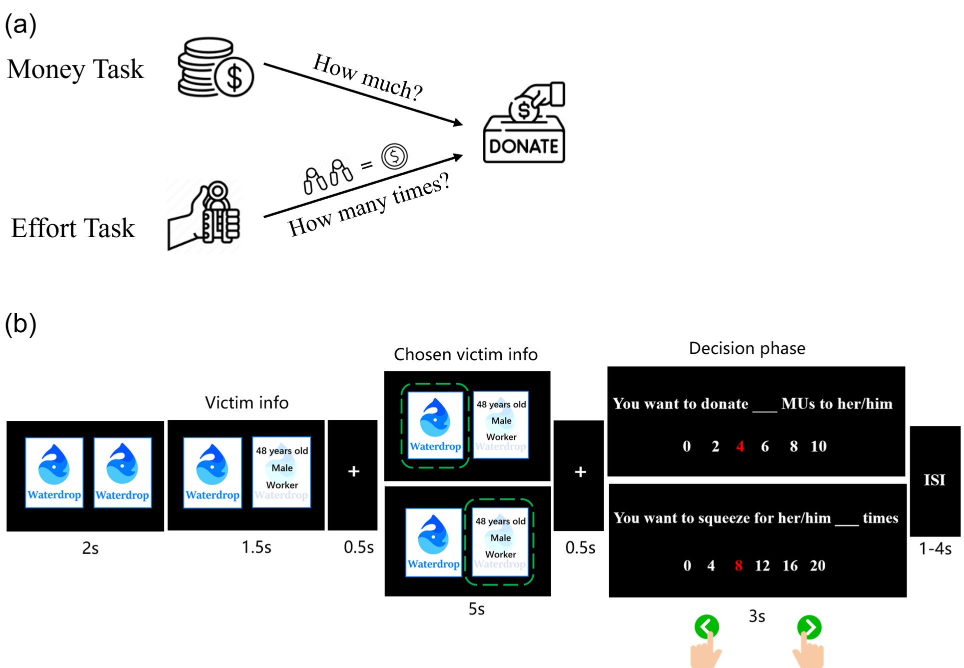

FIGURE 1 Experimental design and procedure. (a) Experimental setting of the two tasks. *Money Task*: Participants were tasked with deciding the amount of monetary units (MUs, use the symbol "$" to indicate.) they wished to donate. Each MU could later be exchanged for additional real money. *Effort Task*: The donation mechanism differed here. Participants donated by squeezing a hand gripper, with every two successful squeezes translating into the donation of 1 MU. They had to decide the number of squeezes they were willing to perform. (b) Schematic of a trial. The event for brain-imaging analysis is marked with a red rectangle (i.e., Chosen victim info). The upper part of the Chosen victim info represented the *UIV condition*, while the lower part represented the *IV condition*. The upper part of the Decision phase represented the decision cues for the Money task, while the lower part was for the Effort task. MU means money units, which could be exchanged for additional money.

donate 1 MU. The squeezing standard was established at 25 kg for male participants and 15 kg for female participants. This meant that, for instance, if a participant chose to squeeze the hand gripper eight times, the corresponding amount for 4 MUs would be donated to the chosen victim. Before initiating the task, each participant performed five grips to familiarize themselves with the sensation of squeezing. In the decision-making phase, participants chose the number of squeezes they were willing to perform to generate MUs for helping the victim. The range of choices varied from 0 to 20 squeezes in increments of 4, which correlated with the donation of 0 to 10 MUs in increments of 2, as in the Money Task (illustrated in Figure 1a).

Consistent with the Money Task, only 12 trials from the Effort Task would be randomly selected for execution. To avoid motion artifacts and preserve the independence of trials, no physical squeezing occurred during the scanning. After the task, participants were informed about the selected trials. They then performed the total number of squeezes accumulated from these trials, and the corresponding monetary amount was donated accordingly.

2.3 | Neuroimaging data acquisition and preprocessing

The data collection and preprocessing procedures were identical for both tasks. MRI data were acquired using a Siemens Prisma 3.0 T MRI machine at the Imaging Center for Brain Research at Shenzhen University. Functional volumes were acquired using multiple slice T2-weighted echo planar imaging sequences with the following parameters: repetition time = 1500 ms, echo time = 30 ms, flip angle = 75°, field of view = 192 × 192 mm^2, 72 slices covering the entire brain, slice thickness = 2 mm, and voxel size = 2 × 2 × 2 mm^3.

fMRI data were preprocessed in SPM12 (Wellcome Department of Imaging Neuroscience, University College London; http://www.fil.ion.ucl.ac.uk/spm). Images were slice-time corrected, motion corrected, and normalized to the Montreal Neurological Institute (MNI) space for each individual with a spatial resolution of 2 × 2 × 2 mm^3. Images were then smoothed using an isotropic Gaussian kernel of 6 mm. Besides, the fMRI data were not normalized and smoothed for multivoxel pattern analysis (MVPA) in the preprocessing steps.

2.4 | Neuroimaging data analysis

2.4.1 | General linear model

For both tasks, identical data analysis procedures were conducted. First, the general linear model (GLM) was established as described by Friston et al. (1995). Regressors were created by convolving a series of functions that represented the sequence of individual events with the default SPM basis function. Alongside the two levels of identifiability (i.e., identifiable and unidentifiable), event type-specific regressors were incorporated to account for BOLD responses related to omission trials. The presentation of victim's information, chosen victim info, decision phase, and the interstimulus interval were modeled as separate regressors in the GLM at the single-participant level. The GLM also included the six rigid-body motion parameters obtained during motion correction to account for motion-related confounds. After establishing GLMs separately for the two tasks, we performed a conjunction analysis in the second-level analysis. This conjunction analysis aimed to uncover the results of whole-brain activation for the identifiable victim effect across the two tasks. This analysis only focused on the "chosen victim info" stage, meaning that only the difference between the IV and UIV conditions at this particular phase was taken into analysis. This analysis reflects a specific decision-making event. We chose the "chosen victim info" stage because the participants would receive all the information they can use for decision-making and have enough time (5 s) to decide. They would make up their minds at this stage, so this stage would reflect the donation decision-making process. For all reported results, the voxel-level significance threshold was set at $p < .001$ uncorrected, with a cluster extent threshold of $k > 20$. False discovery rate (FDR) correction was applied at the cluster level to maintain a significance level of $p < .05$.

2.4.2 | Multivoxel pattern analysis

MVPA allows us to understand what specific information is represented within these regions. Initially, the preprocessed data that had not undergone standardization and smoothing was used. "The Decoding Toolbox" (TDT) facilitated the training and testing of classifiers, along with cross-validation, based on the designed regions of interest (ROIs') patterns of brain activity. Regions that exhibited significant activation in both tasks were selected as ROI, including the MNI coordinates [−52 −44 44] for left TPJ (lTPJ), [52 −46 40] for right TPJ (rTPJ), [30 36 36] for middle frontal gyrus (MFG) in the contrast of (*UIV condition – IV condition*), while [−60 −6 −18] for left MTG (lMTG), [60 −2 −22] for right MTG (rMTG), [−40 16 −38] for TP and MTG in the contrast of (*IV condition – UIV condition*). For each participant and each condition, the mean parameter estimates were computed within a spherical region (radius = 6 mm) centered on these six brain regions.

The brain activity patterns (beta maps) were extracted for each participant under each trial from above mentioned six ROIs. Subsequently, training and testing matrices were designed based on six ROIs mentioned above for classifier training. The classifier could effectively distinguish the activation patterns of the six ROIs between *IV and UIV conditions*. The *p* value of decoding accuracies was estimated by permutation tests. Classifications were performed with shuffled labels for 1000 times to obtain a null distribution. The formula to compute *p* values is as follows: $p = (\text{ranking} + 1)/(\text{number of permutation})$. Additionally, statistical significance was assessed by testing decoding accuracy values across participants for each ROI (chance level was 50% for two conditions) using FDR correction (for the number of ROIs). After classifier training, testing, and cross-validation, individual-level results for the decoding accuracy for *IV and UIV conditions* across the six ROIs could be obtained. Subsequently, group-level analyses were conducted.

2.4.3 | ROI analysis

To test our hypothesized that identifiable victims may induce higher levels of emotional contagion and empathy concern, we selected ROIs from a previous meta-analysis concerning affective empathy; namely, MNI coordinate [−2 23 40] for medial cingulate cortex (MCC), MNI coordinate [−40 22 0] for left insula, and MNI coordinate [39 23 −4] for right insula (Lamm et al., 2011). We then performed one-sample *t* test on the exacted values in the contrast of (*IV condition* > *UIV condition*) to examine whether they were significantly different from zero.

2.4.4 | Functional connectivity analysis (psychophysiological interaction)

We observed that the bilateral TPJ could significantly predict the behavioral index, that is, the identifiable victim effect (i.e., MUs/squeezes donated under IV condition minus MUs/squeezes donated under UIV condition) not only in terms of activation intensity but also in activation patterns. To further explore whether and how the bilateral TPJ interacts with other brain regions during decision-making, we performed psychophysiological interaction (PPI) analysis (Friston et al., 1997) with the bilateral TPJ, MNI [−52 −44 44] for the lTPJ and MNI [52 −46 40] for the rTPJ as seed regions, separately. This analysis allowed us to investigate the dynamic interplay between the bilateral TPJ and other brain areas.

In the PPI analysis, the mean time series of the two seed regions for each participant were initially extracted and adjusted using the F-contrast for the regressors. Subsequently, the peak voxel coordinates within the two ROIs were designated as reference points. Following that, a search was carried out for individual peak voxels around these reference points within a 6-mm radius, employing the contrast of (*IV condition* − *UIV condition*) and (*UIV condition* − *IV condition*), and both utilizing a significance threshold of $p < .001$. This analysis was carried out separately for both rTPJ and lTPJ. The PPI regressors were as follows: (1) the main effect of the contrast (*IV condition* − *UIV condition*) and (*UIV condition* − *IV condition*), (2) the main effect of the activity of seed region, and (3) the interaction of the first two. The regressors above respectively corresponded to PPI.Y, PPI.P, and PPI.ppi in the GLM. Meanwhile, the design matrix also contained the six head-motion parameters as covariates to regress out the impact of head motion. Low-frequency drifts in signal were removed using a high-pass filter with a cutoff at 128 s.

3 | RESULTS

3.1 | Behavioral results

In the Money task, the amount of MUs donated was calculated as the dependent variable. Paired *t* test revealed that when facing an identifiable victim, individuals demonstrated significantly a higher prosocial tendency toward an identifiable victim compared to an unidentifiable victim (5.43 ± 1.89 vs. 4.35 ± 1.92 [mean ± SE], t (30) = 6.96, $p < .01$, Cohen's $d = 0.57$) (Figure 2a).

In the Effort task, the number of squeezes participants were willing to take was calculated as the dependent variable. Paired *t* test revealed that individuals demonstrated significantly a higher prosocial tendency toward an identifiable victim compared to an unidentifiable victim (10.17 ± 4.426 vs. 8.16 ± 4.72, t (30) = 6.42, $p < .01$, Cohen's $d = 0.44$) (Figure 2b).

Then, we calculated the difference between the MUs/squeezes donated for IV and UIV and used it as the behavioral index of the “identifiable victim effect”. This index reflected the difference in prosocial tendency between IV and UIV conditions. For the Money task, the behavioral index was 1.08 ± 0.86, while a one-sample *t* test revealed that the behavioral index was significantly greater than 0 (t (30) = 6.96, $p < .001$, Cohen's $d = 1.77$). For the Effort task, this index was 2.01 ± 1.74, while a one-sample *t* test revealed that the behavioral index was significantly greater than 0 (t (30) = 6.42, $p < .001$, Cohen's $d = 1.63$). Both tasks revealed a significant “identifiable victim effect” (Figure 2a,b). Further, a correlation analysis was conducted on both tasks. The results revealed a significant positive correlation between the two ($r = .74$, $p < .001$) (Figure 2c).

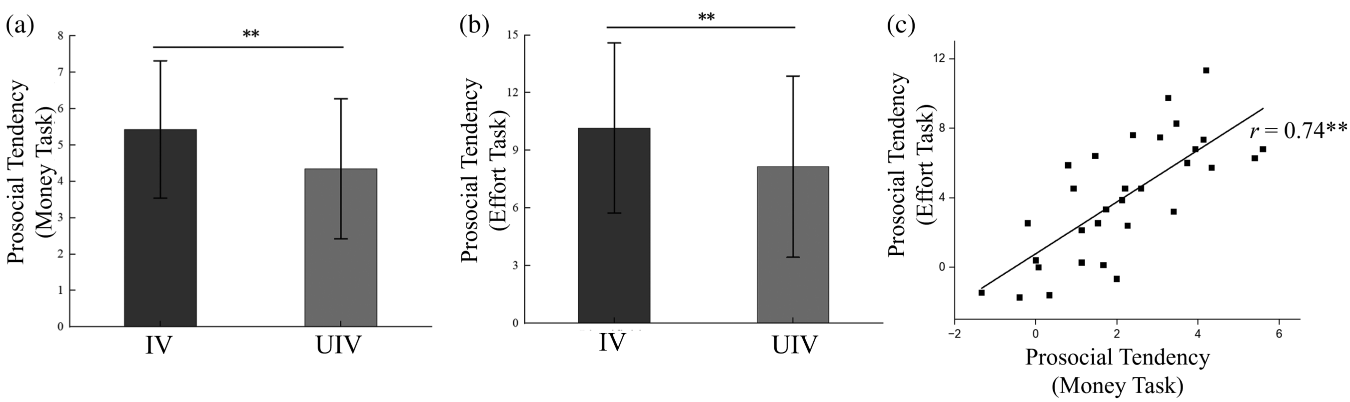

FIGURE 2 Behavioral results. (a) Behavioral results of the Money Task. (b) Behavioral results of the Effort Task. **: $p < .01$. ***: $p < .001$ (c) Result of the correlation analysis between the behavioral index of “identifiable victim effect” in the Money task and the Effort task. **: $p < .01$.

3.2 | General linear model

The whole-brain activation results of the two tasks revealed a high degree of consistency in the significantly activated brain regions (for details of activations in each task, please see Tables S1 and S2). A conjunction analysis was performed utilizing the data from both tasks.

The results of the conjunction analysis showed that the main contrast of (*IV condition* > *UIV condition*) revealed activation in the lmPFC (MNI [−10 44 48]), lMTG (MNI [−60 −6 −18]), TP: superior temporal gyrus (MNI [−42 22 −16]), posterior cingulate cortex (MNI [−4 −50 24]), rMTG (MNI [60 −2 −22]), right orbital part of inferior frontal gyrus (orbIFG, MNI [32 30 −16]), right dorsolateral superior frontal gyrus (dorSFG, MNI [20 40 52]), left TP: middle temporal gyrus (MNI [−40 16 −38]). The reversed contrast of (*UIV condition* > *IV condition*) revealed activation in the rTPJ (MNI [52 −46 40]), lTPJ (MNI [−52 −44 44]), rMFG (MNI [30 36 36]), lMTG (MNI [−44 −68 10]), right precental gyrus (PCG, MNI [38 6 48]), left dorsolateral superior frontal gyrus (dorSFG, MNI [−20 8 62]), right medial cingulate and paracingulate gyrus (MCG, MNI [8 −24 46]) (Figure 3 and Table 1). All the results reported above were significant at $p < .001$, $k > 20$ voxels, cluster-level FDR correction at $p < .05$.

3.3 | MVPA analysis

Six ROIs with the highest activations within the contrast between *IV and UIV conditions*, including lTPJ, rTPJ, MFG in the contrast of (*UIV condition* – *IV condition*) and lMTG, rMTG, TP in the contrast of (*IV condition* – *UIV condition*) were defined as ROI for MVPA analysis (Table 2 and Figure 4a).

MVPA analysis revealed that these six ROIs could significantly classify between identifiable victim trials and unidentifiable victim trials in the 1000 permutation (classification accuracy in Money Task: ACC(lTPJ) = 64.32%, $p < .001$; ACC(rTPJ) = 65.54%, $p < .001$; ACC(MFG) = 55.34%, $p = .01$; ACC(lMTG) = 61.26%, $p < .001$; ACC(rMTG) = 62.01%, $p < .001$; ACC(TP) = 56.50%, $p < .001$; Effort Task: ACC(lTPJ) = 65.85%, $p < .001$; ACC(rTPJ) = 59.97%, $p = .005$; ACC(MFG) = 59.04%, $p < .001$; ACC(lMTG) = 60.99%, $p < .001$; ACC(rMTG) = 56.84%, $p = .006$; ACC(TP) = 58.78%, $p = .001$) (Figure 4b).

3.4 | ROI analysis

To test our hypothesis that an identifiable victim may induce a higher level of emotional contagion and empathy concern, we selected three

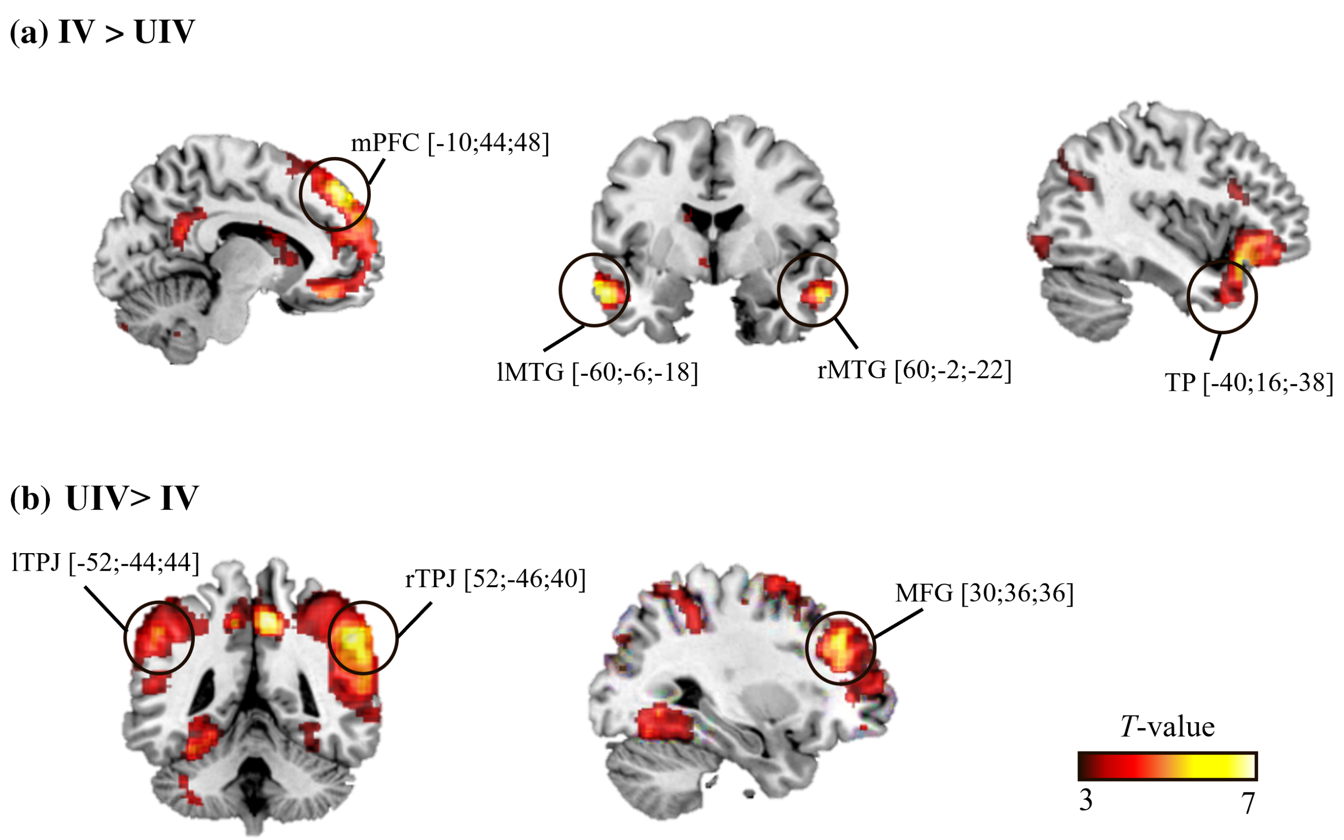

FIGURE 3 Results of brain activation in conjunction analysis. (a) Brain activation of *IV condition* > *UIV condition*. (b) Brain activation of the contrast of *UIV condition* > *IV condition*. lMTG, left middle temporal gyrus; lTPJ, left temporoparietal junction; MFG, middle frontal gyrus; mPFC, medial superior frontal gyrus; rMTG, right middle temporal gyrus; rTPJ, right temporoparietal junction; TP, temporal pole: middle temporal gyrus.

TABLE 1 Whole-brain activations based on the conjunction analysis results.

Brain region	BA	Coordinates (X, Y, Z)			Vol.	T value
IV condition > UIV condition						
Left medial prefrontal cortex	9	−10	44	48	2010	8.45
		−6	52	44		7.72
		−4	54	20		7.44
Left middle temporal gyrus	21	−60	−6	−18	402	7.28
Left temporal pole: superior temporal gyrus	38	−42	22	−16	957	7.05
		−42	26	−8		6.96
		−28	18	−18		6.54
Posterior cingulate cortex	30	−4	−50	24	648	6.86
		−4	−40	34		6.29
		4	−52	26		6.09
Right middle temporal gyrus	21	60	−2	−22	146	6.29
Right orbital part of inferior frontal gyrus	47	32	30	−16	153	6.18
		42	22	−14		5.66
Right dorsolateral superior frontal gyrus	9	20	40	52	89	5.39
		12	46	48		5.06
Left temporal pole: middle temporal gyrus	20	−40	16	−38	23	5.04
UIV condition > IV condition						
Right temporoparietal junction	40	52	−46	40	2961	8.18
		64	−38	30		7.44
		48	−40	20		6.99
Left temporoparietal junction	40	−52	−44	44	1081	6.41
		−54	−32	38		6.07
		−54	−34	48		5.87
Right middle frontal gyrus	9	30	36	36	741	6.30
		30	36	22		6.09
		32	30	28		5.43
Left middle temporal gyrus	37	−44	−68	10	515	5.99
		−44	−78	16		5.62
		−56	−66	2		5.14
Right precentral gyrus	6	38	6	48	69	5.43
		48	2	48		4.39
Left dorsolateral superior frontal gyrus	6	−20	8	62	45	5.02
		−24	2	56		4.25
Right medial cingulate and paracingulate gyrus		8	−24	46	34	5.01

Note: all the results reported above were significant at $p < .001$, $k > 20$ voxels, cluster-level FDR correction at $p < .05$.
Abbreviations: FDR, false discovery rate; IV, identifiable victim; UIV, unidentifiable victim.

ROIs from a previous meta-analysis concerning affective empathy (Lamm et al., 2011). One-sample t tests on the exacted values in the contrast of (*IV condition* > *UIV condition*) revealed that in both the Money task and Effort task, the left insula was significantly larger than zero (Money task: 0.94 ± 1.75, t (30) = 2.99, $p = .006$; Effort task: 0.94 ± 2.06, t (30) = 2.55, $p = .016$). MCC was significantly larger than zero in Effort task, but not in Money task (Money task: 0.32 ± 2.14, t (30) = 0.84, $p = .41$; Effort task: 1.01 ± 2.25, t (30) = 2.50, $p = .018$), while right insula was significantly in Money task, but not in Effort task (Money task: 0.55 ± 1.39, t (30) = 2.22, $p = .034$; Effort task: 0.55 ± 1.63, t (30) = 1.88, $p = .07$).

Besides, from the results of MVPA, we observed that in both tasks, the classification accuracy of the bilateral TPJ ranked the highest. This suggests that in both tasks, the bilateral TPJ can significantly distinguish between identifiable and unidentifiable conditions. To explore the relationship between bilateral TPJ activation and

TABLE 2 The ROIs defined by activation in the conjunction analysis.

Brain region	MNI coordinates x	y	z
1. Left temporoparietal junction	−52	−44	44
2. Right temporoparietal junction	52	−46	40
3. Middle frontal gyrus	30	36	36
4. Left middle temporal gyrus	−60	−6	−18
5. Right middle temporal gyrus	60	−2	−22
6. Temporal pole: middle temporal gyrus	−40	16	−38

Abbreviations: MNI, Montreal Neurological Institute; ROI, region of interest.

identifiable victim effect, Pearson's correlation analysis was separately computed in both tasks, all of which were measured in the contrast of (*IV condition* > *UIV condition*). The results revealed that irrespective of the Money Task or Effort Task, lTPJ activation exhibited a significant negative correlation with identifiable victim effect index (Money Task: $r = -.38$, $p = .035$; Effort Task: $r = -.40$, $p = .024$). Additionally, in both tasks, rTPJ demonstrated a trend of negative correlation with identifiable victim effect index (Money Task: $r = -.32$, $p = .077$; Effort Task: $r = -.34$, $p = .058$) (Figure 4c,d).

3.5 | PPI analysis

For the rTPJ seed region, significant functional connectivity between rTPJ and mPFC was detected in both tasks (Money task: peak MNI [4 32 2], cluster size = 31, t (30) = 4.34; Effort task: peak MNI [4 30 10], cluster size = 1407, t (30) = 7.19) in the contrast of (*IV condition* – *UIV condition*) but not (*UIV condition* – *IV condition*) (Figure 5). For the seed region of the lTPJ, significant shared functional connections in the (*IV condition* – *UIV condition*) or (*UIV condition* – *IV condition*) contrast for both tasks were not observed. All the results reported above were significant at $p < .001$, $k > 20$ voxels, cluster-level FDR correction at $p < .05$.

4 | DISCUSSION

The present study examined how individuals' prosocial decision-making is modulated by the identifiability of the victims. In a novel approach, we leveraged real-life scenarios from an actual online donation platform, namely "Waterdrop." This choice was instrumental in enhancing the ecological validity of our study, as participants were cognizant that the victims they encountered were real individuals confronting serious life challenges. To further solidify the reliability and robustness of our findings, we designed and executed two separate tasks within the study framework.

Behaviorally, both tasks displayed consistent results. The nature of the helping cost, whether monetary or physical, did not significantly alter prosocial decisions. This finding aligns with existing literature, demonstrating a marked identifiable victim effect across both tasks. Participants consistently showed a preference for aiding identifiable victims over unidentifiable ones.

On the neural level, we observed a high degree of consistency between the two tasks. Firstly, we found that when the victim was identifiable, stronger activation in the mPFC was observed than when the victim was unidentifiable. The mPFC is a brain region deeply entwined with networks responsible for value assessment and decision-making processes (Rushworth et al., 2011), which suggests that when participants were presented with identifiable victims, they engaged more intensively in the cognitive processing of the victim's information. This processing likely involved assessing the value and impact of the help being considered. In comparison to unidentifiable victims, identifiable victims, armed with more personal information, were seemingly more successful in capturing the decision-makers' attention and eliciting a more pronounced valuation in the decision-making process. This is consistent with previous findings (Dickert, 2008; Jenni & Loewenstein, 1997; Peters et al., 2003).

The whole-brain analysis did not reveal stronger activation in regions traditionally associated with affective empathy, such as the insula and MCC. However, when we directed our focus to a more detailed ROI analysis, we uncovered that the left insula, a region associated with affective empathy, showed a heightened activation in scenarios involving an identifiable victim. This finding in both tasks lends partial support to our hypothesis positing that identifiable victims are likely to trigger stronger affective empathy responses in individuals.

Conversely, when the victim was unidentifiable, we found stronger activation in the bilateral TPJ. This observation may indicate that when dealing with unidentifiable and vague victims, participants had to invest additional effort in the mentalizing process. Mentalizing, or cognitive empathy, involves the capacity to speculate and understand the needs and emotional states of others, a process that is essential for making informed and empathetic decisions (Samson et al., 2004). An alternative explanation for the increased activation in the bilateral TPJ might be that it reflects an intensified effort to reduce social distance with strangers when engaging in helping decisions. Prior research has shown that activation in the TPJ is closely linked with levels of generosity, particularly in contexts involving strangers (Sellitto et al., 2021; Strombach et al., 2015). Thus, in the context of unidentifiable victims, the TPJ activation could signify an individual's cognitive and emotional struggle to transcend inherent self-centered tendencies, thereby facilitating a more prosocial and altruistic behavior. The greater the TPJ activation, the less pronounced the identifiable victim effect appeared to be.

This relationship was further elucidated through our correlation analysis, which revealed a negative correlation between TPJ activation and the strength of the identifiable victim effect. In essence, heightened activity in the TPJ, a region linked with cognitive empathetic processing (Morishima et al., 2012; Tusche et al., 2016), was associated with a diminished identifiable victim effect. This aligns with a body of literature suggesting that empathetic responses play a significant role in shaping prosocial decision-making behaviors (Davis, 1983;

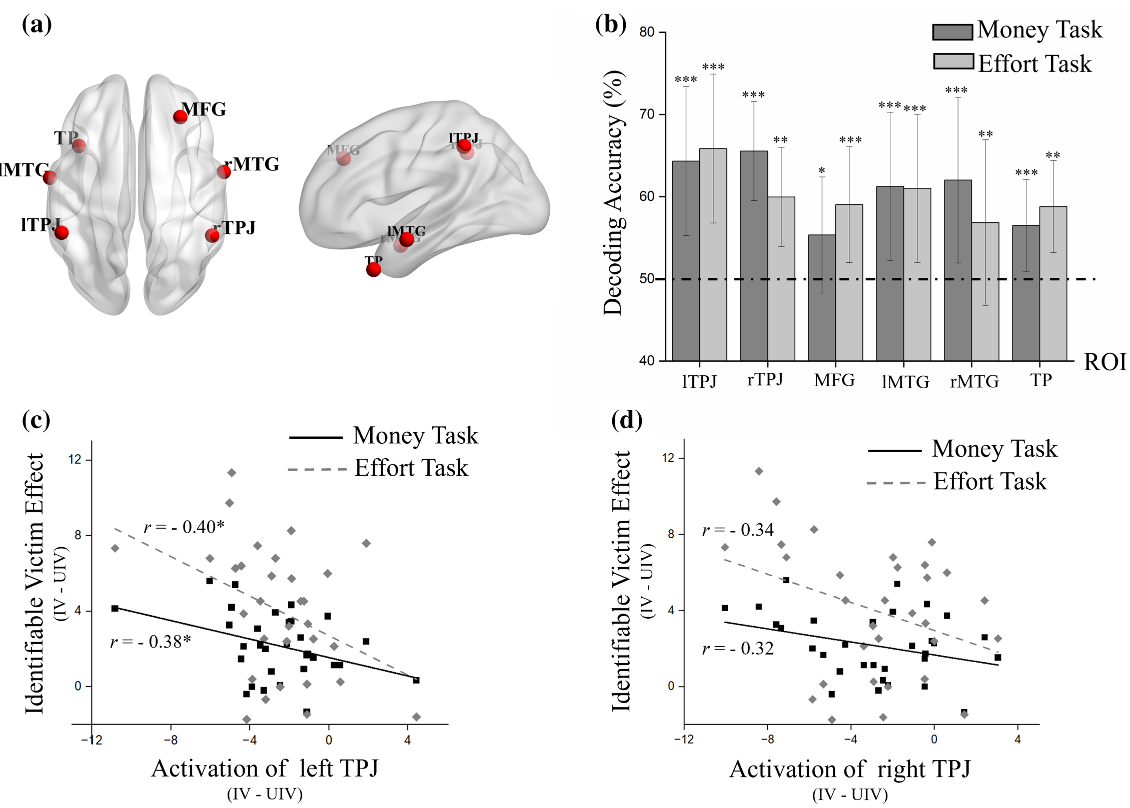

FIGURE 4 MVPA and ROI analysis results. (a) The position of six ROIs on the brain. (b) MVPA results (i.e., regions that significantly classify between identifiable victim trials and unidentifiable victim trials in two tasks). *: $p < .05$, **: $p < .01$, ***: $p < .001$. (c) The correlation between lTPJ activation and identifiable victim effect separately for two tasks. *: $p < .05$. (d) The correlation between rTPJ activation and identifiable victim effect separately for two tasks. lTPJ, left temporoparietal junction; rTPJ, right temporoparietal junction; MVPA, multivoxel pattern analysis; ROI, region of interest.

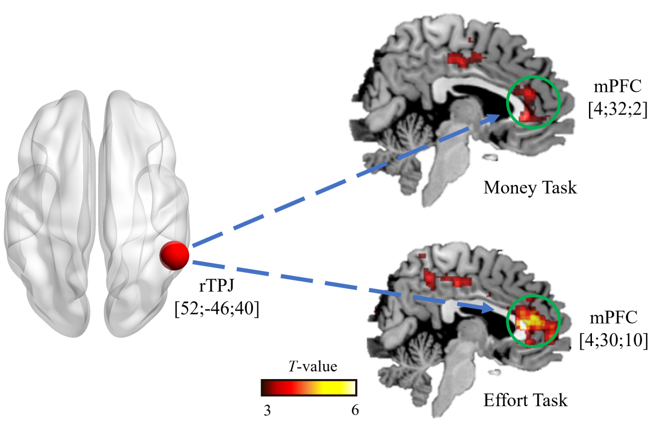

FIGURE 5 PPI results. Both tasks presented consistent PPI results: the functional connectivity between rTPJ and mPFC was significant for the contrast of (*IV condition > UIV condition*). mPFC, medial prefrontal cortex; PPI, psychophysiological interaction; rTPJ, right temporoparietal junction.

Gladstein, 1983; Kogut & Ritov, 2005; Mai et al., 2016; Miller et al., 2020; Tusche et al., 2016). Some studies have even noted that the presence of an identifiable victim can increase an individual's willingness to donate by inducing a stronger empathetic response (Kogut & Ritov, 2005; Xing et al., 2015). Thus, our findings suggest that the TPJ activation is indicative of a more rigorous mentalizing and empathizing process that participants engage in when confronted with the plight of unidentifiable victims.

Using MVPA, it was found significant differences in activation patterns within these ROIs when comparing identifiable and unidentifiable trials, which shed light on the differential processing that occurs in the brain based on the level of victim identifiability. Further, PPI analysis, which employed the rTPJ as a seed region, indicated that the strength of functional connectivity between the rTPJ and mPFC varied in accordance with the identifiable victim effect. This variation was consistent across both the Money Task and the Effort Task. The TPJ and mPFC are both integral to the mentalizing network, with the mPFC playing a significant role in the decision-making process (Bault et al., 2011; Bzdok et al., 2012; Denny et al., 2012; Mars et al., 2012; Van Overwalle, 2009). The PPI results may suggest that the identifiability of victims influences the valuation process of decision-making, as reflected in the activation of mPFC through its modulation of mentalizing process, as reflected in the activation of TPJ. The more one can mentalize with the unidentifiable victim, the stronger the functional connection between the TPJ and mPFC, and the weaker the observed identifiable victim effect. On the other hand, when participants were presented with identifiable victims, the provided information potentially facilitated their ability to effectively empathize with the victims' feelings and pain, leading to enhanced prosocial tendency. This aligns with previous research suggesting that concrete, relatable information about victims can enhance empathetic responses and prosocial behavior (Ein-Gar & Levontin, 2013; Kim et al., 2008; Liviatan et al., 2008). The observed connection between the TPJ and mPFC in both the Money Task and the Effort Task could be crucial in understanding the underlying neural mechanisms that influence how identifiability biases decision preferences.

In summary, through two tasks, the present study revealed consistent behavioral and neural results of significant identifiable victim effects in prosocial decision-making. Behaviorally, it was found that across different forms of helping cost, the effect was preserved and highly stable. Neurally, the effect was closely linked to the bilateral, especially the rTPJ. When the personal information of victims is unknown, the heightened activation of rTPJ may reflect a higher level of mentalizing process to a vague victim, and the effect of TPJ further modulates the valuation process through its functional connectivity with the mPFC.

It is important to acknowledge the limitations of this study. First, Prior research has highlighted that identifiable victims can significantly influence decision-making through the emotional responses they evoke. In our study, activations in areas typically associated with emotional responses were not prominently observed. This could be attributed to the relatively limited and less vivid nature of the information about the victims provided through online donation platforms, potentially hindering the ability to evoke strong emotional responses in participants. This observation is consistent with the noted high level of involvement of mentalizing (cognitive empathy) regions. Future studies employing more vivid and emotionally evocative stimuli, such as pictures and videos, may help to address this issue. Second, subsequent research might benefit from incorporating additional factors that influence prosocial decision-making, such as the urgency of the assistance request. Exploring how the identifiable victim effect manifests under varying degrees of urgency could provide a more nuanced understanding of its impact, enhancing our comprehension of the dynamics at play in prosocial behaviors and decision-making processes.

AUTHOR CONTRIBUTIONS

FC conceived the study; HZ and YX conducted the experiments and collected data; HZ, JL, and YX analyzed data; HZ and FC wrote the paper; FC, LL, and JL reviewed the manuscript.

ACKNOWLEDGMENTS

This work was supported by the National Natural Science Foundation of China (no. 32171013) and the Science and Technology Innovation Commission of Shenzhen (grant/award number JCYJ20210308103903001). We thank Dr Q.H. Yue for proofreading the manuscript.

CONFLICT OF INTEREST STATEMENT

The authors declare no conflicts of interest.

DATA AVAILABILITY STATEMENT

Data sets are available on the Science Data Bank (https://www.scidb.cn/s/YjY32q). Further inquiries can be directed to the first author, Hailing Zhao (zhaohailing2021@email.szu.edu.cn).

ORCID

Jie Liu https://orcid.org/0000-0001-8874-7499
Fang Cui https://orcid.org/0000-0003-4487-8790

REFERENCES

Andreoni, J. (1990). Impure altruism and donations to public goods: A theory of warm-glow giving. *The Economic Journal*, *100*(401), 464. https://doi.org/10.2307/2234133

Bartra, O., McGuire, J. T., & Kable, J. W. (2013). The valuation system: A coordinate-based meta-analysis of BOLD fMRI experiments examining neural correlates of subjective value. *NeuroImage*, *76*, 412–427.

Bault, N., Joffily, M., Rustichini, A., & Coricelli, G. (2011). Medial prefrontal cortex and striatum mediate the influence of social comparison on the decision process. *Proceedings of the National Academy of Sciences of the United States of America*, *108*(38), 16044–16049. https://doi.org/10.1073/pnas.1100892108

Buckner, R. L., Andrews-Hanna, J. R., & Schacter, D. L. (2008). The Brain's default network: Anatomy, function, and relevance to disease. *Annals of the New York Academy of Sciences*, *1124*(1), 1–38. https://doi.org/10.1196/annals.1440.011

Bzdok, D., Schilbach, L., Vogeley, K., Schneider, K., Laird, A. R., Langner, R., & Eickhoff, S. B. (2012). Parsing the neural correlates of moral cognition: ALE meta-analysis on morality, theory of mind, and empathy. *Brain Structure and Function*, *217*(4), 783–796.

Corbetta, M., Patel, G., & Shulman, G. L. (2008). The reorienting system of the human brain: From environment to theory of mind. *Neuron*, *58*(3), 306–324. https://doi.org/10.1016/j.neuron.2008.04.017

Davis, M. H. (1983). Measuring individual differences in empathy: Evidence for a multidimensional approach. *Journal of Personality and Social Psychology*, *44*(1), 113–126. https://doi.org/10.1037/0022-3514.44.1.113

Decety, J., & Lamm, C. (2007). The role of the right temporoparietal junction in social interaction: How low-level computational processes contribute to meta-cognition. *The Neuroscientist*, *13*(6), 580–593. https://doi.org/10.1177/1073858407304654

Denny, B. T., Kober, H., Wager, T. D., & Ochsner, K. N. (2012). A meta-analysis of functional neuroimaging studies of self- and other judgments reveals a spatial gradient for mentalizing in medial prefrontal cortex. *Journal of Cognitive Neuroscience*, *24*(8), 1742–1752. https://doi.org/10.1162/jocn_a_00233

Dickert, S. (2008). *Attentional mechanisms in the generation of sympathy—All databases*. https://webofscience.clarivate.cn/wos/alldb/full-record/WOS:000259264303144

Dickert, S., Sagara, N., & Slovic, P. (2011). Affective motivations to help others: A two-stage model of donation decisions. *Journal of Behavioral Decision Making*, *24*(4), 361–376. https://doi.org/10.1002/bdm.697

Ein-Gar, D., & Levontin, L. (2013). Giving from a distance: Putting the charitable organization at the center of the donation appeal. *Journal of Consumer Psychology*, *23*(2), 197–211. https://doi.org/10.1016/j.jcps.2012.09.002

Erlandsson, A., Björklund, F., & Bäckström, M. (2015). Emotional reactions, perceived impact and perceived responsibility mediate the identifiable victim effect, proportion dominance effect and in-group effect respectively. *Organizational Behavior and Human Decision Processes*, *127*, 1–14. https://doi.org/10.1016/j.obhdp.2014.11.003

Fetherstonhaugh, D., Slovic, P., & Johnson, S. (1997). Insensitivity to the value of human life: A study of psychophysical numbing. *Journal of Risk and Uncertainty*, *14*, 283–300. https://doi.org/10.1023/A:1007744326393

Friston, K. J., Buechel, C., Fink, G. R., Morris, J., Rolls, E., & Dolan, R. J. (1997). Psychophysiological and modulatory interactions in neuroimaging. *NeuroImage*, *6*(3), 218–229. https://doi.org/10.1006/nimg.1997.0291

Friston, K., Holmes, A., Worsley, K., Poline, J. B., Frith, C., & Frackowiak, R. (1995). Statistical parametric maps in functional imaging: a general linear approach. *Human Brain Mapping*, *2*, 189–210. https://doi.org/10.1002/hbm.460020402

Frith, C. D., & Singer, T. (2008). The role of social cognition in decision making. *Philosophical Transactions of the Royal Society B: Biological Sciences*, *363*(1511), 3875–3886. https://doi.org/10.1098/rstb.2008.0156

Genevsky, A., Västfjäll, D., Slovic, P., & Knutson, B. (2013). Neural underpinnings of the identifiable victim effect: Affect shifts preferences for giving. *The Journal of Neuroscience*, *33*(43), 17188–17196. https://doi.org/10.1523/JNEUROSCI.2348-13.2013

Gladstein, G. A. (1983). Understanding empathy: Integrating counseling, developmental, and social psychology perspectives. *Journal of Counseling Psychology*, *30*(4), 467–482. https://doi.org/10.1037/0022-0167.30.4.467

Harbaugh, W. T., Mayr, U., & Burghart, D. R. (2007). Neural responses to taxation and voluntary giving reveal motives for charitable donations. *Science*, *316*(5831), 1622–1625. https://doi.org/10.1126/science.1140738

Hou, J., Zhang, C., Zhao, F., & Guo, H. (2023). Underlying mechanism to the identifiable victim effect in collective donation action intentions: Does emotional reactions and perceived responsibility matter? *VOLUNTAS: International Journal of Voluntary and Nonprofit Organizations*, *34*, 552–572. https://doi.org/10.1007/s11266-022-00480-9

Jenni, K. E., & Loewenstein, G. (1997). *Explaining the "identifiable victim effect"*.

Kim, K., Zhang, M., & Li, X. (2008). Effects of temporal and social distance on consumer evaluations: Table 1. *Journal of Consumer Research*, *35*(4), 706–713. https://doi.org/10.1086/592131

Kogut, T., & Kogut, E. (2011). Possession attachment: Individual differences in the endowment effect. *Journal of Behavioral Decision Making*, *24*(4), 377–393. https://doi.org/10.1002/bdm.698

Kogut, T., & Kogut, E. (2013). Exploring the relationship between adult attachment style and the identifiable victim effect in helping behavior. *Journal of Experimental Social Psychology*, *49*(4), 651–660. https://doi.org/10.1016/j.jesp.2013.02.011

Kogut, T., & Ritov, I. (2005). The "identified victim" effect: An identified group, or just a single individual? *Journal of Behavioral Decision Making*, *18*(3), 157–167. https://doi.org/10.1002/bdm.492

Lamm, C., Decety, J., & Singer, T. (2011). Meta-analytic evidence for common and distinct neural networks associated with directly experienced pain and empathy for pain. *NeuroImage*, *54*(3), 2492–2502.

Lee, S., & Feeley, T. H. (2016). The identifiable victim effect: A meta-analytic review. *Social Influence*, *11*(3), 199–215. https://doi.org/10.1080/15534510.2016.1216891

Liviatan, I., Trope, Y., & Liberman, N. (2008). Interpersonal similarity as a social distance dimension: Implications for perception of Others' actions. *Journal of Experimental Social Psychology*, *44*(5), 1256–1269. https://doi.org/10.1016/j.jesp.2008.04.007

Loewenstein, G., & Small, D. A. (2007). The scarecrow and the tin man: The vicissitudes of human sympathy and caring. *Review of General Psychology*, *11*(2), 112–126. https://doi.org/10.1037/1089-2680.11.2.112

Mai, X., Zhang, W., Hu, X., Zhen, Z., Xu, Z., Zhang, J., & Liu, C. (2016). Using tDCS to explore the role of the right temporo-parietal junction in theory of mind and cognitive empathy. *Frontiers in Psychology*, *7*, 380. https://doi.org/10.3389/fpsyg.2016.00380

Mars, R. B., Sallet, J., Schüffelgen, U., Jbabdi, S., Toni, I., & Rushworth, M. F. S. (2012). Connectivity-based subdivisions of the human right "temporoparietal junction area": Evidence for different areas participating in different cortical networks. *Cerebral Cortex (New York, N.Y.: 1991)*, *22*(8), 1894–1903. https://doi.org/10.1093/cercor/bhr268

Miller, J. G., Xia, G., & Hastings, P. D. (2020). Right temporoparietal junction involvement in autonomic responses to the suffering of others: A preliminary transcranial magnetic stimulation study. *Frontiers in Human Neuroscience*, *14*, 7. https://doi.org/10.3389/fnhum.2020.00007

Morishima, Y., Schunk, D., Bruhin, A., Ruff, C. C., & Fehr, E. (2012). Linking brain structure and activation in temporoparietal junction to explain the neurobiology of human altruism. *Neuron*, *75*(1), 73–79. https://doi.org/10.1016/j.neuron.2012.05.021

Peters, E., Slovic, P., & Gregory, R. (2003). The role of affect in the WTA/-WTP disparity. *Journal of Behavioral Decision Making*, *16*(4), 309–330. https://doi.org/10.1002/bdm.448

Rushworth, M. F. S., Noonan, M. P., Boorman, E. D., Walton, M. E., & Behrens, T. E. (2011). Frontal cortex and reward-guided learning and decision-making. *Neuron*, *70*(6), 1054–1069. https://doi.org/10.1016/j.neuron.2011.05.014

Samson, D., Apperly, I. A., Chiavarino, C., & Humphreys, G. W. (2004). Left temporoparietal junction is necessary for representing someone else's belief. *Nature Neuroscience*, *7*(5), 499–500. https://doi.org/10.1038/nn1223

Schurz, M., Radua, J., Aichhorn, M., Richlan, F., & Perner, J. (2014). Fractionating theory of mind: A meta-analysis of functional brain imaging studies. *Neuroscience & Biobehavioral Reviews*, *42*, 9–34. https://doi.org/10.1016/j.neubiorev.2014.01.009

Sellitto, M., Neufang, S., Schweda, A., Weber, B., & Kalenscher, T. (2021). Arbitration between insula and temporoparietal junction subserves framing-induced boosts in generosity during social discounting. *NeuroImage*, *238*, 118211.

Singer, T. (2006). The neuronal basis and ontogeny of empathy and mind reading: Review of literature and implications for future research. *Neuroscience and Biobehavioral Reviews*, *30*(6), 855–863.

Small, D. A., Loewenstein, G., & Slovic, P. (2007). Sympathy and callousness: The impact of deliberative thought on donations to identifiable and statistical victims. *Organizational Behavior and Human Decision Processes*, *102*(2), 143–153. https://doi.org/10.1016/j.obhdp.2006.01.005

Strombach, T., Weber, B., Hangebrauk, Z., Kenning, P., Karipidis, I. I., Tobler, P. N., & Kalenscher, T. (2015). Social discounting involves modulation of neural value signals by temporoparietal junction. *Proceedings of the National Academy of Sciences of the United States of America*, *112*(5), 1619–1624.

Tremblay, S., Sharika, K. M., & Platt, M. L. (2017). Social decision-making and the brain: A comparative perspective. *Trends in Cognitive Sciences*, *21*(4), 265–276. https://doi.org/10.1016/j.tics.2017.01.007

Tusche, A., Böckler, A., Kanske, P., Trautwein, F.-M., & Singer, T. (2016). Decoding the charitable brain: Empathy, perspective taking, and attention shifts differentially predict altruistic giving. *The Journal of Neuroscience*, *36*(17), 4719–4732. https://doi.org/10.1523/JNEUROSCI.3392-15.2016

Van Overwalle, F. (2009). Social cognition and the brain: A meta-analysis. *Human Brain Mapping*, *30*(3), 829–858. https://doi.org/10.1002/hbm.20547

Van Overwalle, F., & Baetens, K. (2009). Understanding others' actions and goals by mirror and mentalizing systems: A meta-analysis.

NeuroImage, *48*(3), 564–584. https://doi.org/10.1016/j.neuroimage.2009.06.009

Xing, S., Yuan, M., Sun, L., & Lin, C. (2015). The effects and mechanism of dispositional empathy and victim Identifi ability on college Students' willingness of donation. *Journal of Psychological Science*, *38*(4), 870–875. https://doi.org/10.16719/j.cnki.1671-6981.2015.04.014

Young, L., Cushman, F., Hauser, M., & Saxe, R. (2007). The neural basis of the interaction between theory of mind and moral judgment. *Proceedings of the National Academy of Sciences of the United States of America*, *104*(20), 8235–8240. https://doi.org/10.1073/pnas.0701408104

SUPPORTING INFORMATION

Additional supporting information can be found online in the Supporting Information section at the end of this article.

How to cite this article: Zhao, H., Xu, Y., Li, L., Liu, J., & Cui, F. (2024). The neural mechanisms of identifiable victim effect in prosocial decision-making. *Human Brain Mapping*, *45*(2), e26609. https://doi.org/10.1002/hbm.26609